Estimation of temperature dependent equivalent circuit parameters for traction-based electric machines

Agbaje, O., Kavanagh, D.F., Sumisławska, M., Howey, D.A., McCulloch, M.D., and Burnham, K.J.

http://dx.doi.org/ 10.1049/cp.2013.1898

Estimation of temperature dependent equivalent circuit parameters for traction-based electric machines

***O. Agbaje*[*,‡], *D.F. Kavanagh*[†], *M. Sumisławska*[*], *D.A. Howey*[†], *M.D. McCulloch*[†], *K.J. Burnham*[*]**

[*]*Department of Mathematics and Control Engineering, Coventry University, UK*
[†]*Department of Engineering Science, University of Oxford, UK*
[‡]*corresponding author, e-mail oluwaleke.agbaje@coventry.ac.uk*

Keywords: equivalent circuit model, impedance response, induction machine

Abstract

The influence of temperature conditions on electric machine models is not well understood. This paper investigates modelling the temperature dependence of equivalent circuit parameters. Experiments have been performed on an induction machine to characterise its impedance response (up to 10 MHz) over the temperature range (22.4-210) ^{o}C. Using these measurements non-linear parameter estimation is performed using the Nelder-Mead method to derive temperature-dependent models, with an average absolute magnitude error of 270 Ω. The accuracy has been evaluated over the frequency range for the different temperatures and highlights where improvements are needed. This work has important applications in electric machine design and condition monitoring. Also it provides a valuable precursor towards developing age-dependent models for traction based applications.

1 Introduction

Electric machine models are useful for describing and predicting the machine's behaviour. The predominant applications for models in this field are in machine design [1, 2], condition monitoring for diagnosis [3, 4], ageing [5], modelling the machine temperature for cooling purposes [6, 7], and for control systems [8].

Different types of models include equivalent circuit models (ECMs) [1, 2], finite element models (FEMs) [1, 2] and equivalent magnetic circuits [2, 9, 10]. ECMs are more common [2] and are based on the lumped RLC parameters of the stator and rotor windings electromagnetic network. The IEEE Standard 112 defines a per-phase low-frequency equivalent circuit model [11] for an induction machine. However, this model is for low-frequency (below the first resonant frequency), hence it contains purely inductive and resistive elements and therefore does not cater for inter-turn capacitance and leakage capacitance between (stator and frame, rotor and stator, rotor and frame). Models presented by G. Grandi et al. [12] and O. A. Mohammed et al. [13] have incorporated high frequency elements to a certain extent. In [12] the turn to turn, turn to iron, stray capacitances, skin and proximity effects, dielectric and iron losses are taken into account in the equivalent circuit of a mush wound AC motor. The work of Mirafzal et al. [14] proposed a universal three phase equivalent circuit model for low and high frequency characteristics of an induction motor by considering lumped winding to winding and winding to frame capacitance parameters and nonlinear high frequency stator voltage gradient effects. More recently, H. Peng et al. [15] proposed a quick method for obtaining an ECM for AC and DC machines from impedance amplitude-frequency characteristic measurements.

Models and studies done by [12, 13, 14, 15] do not take into consideration the extreme working conditions such as high temperatures, humidity and vibration that electric machines are subjected to in aerospace, and automotive applications. Copper losses, iron losses and mechanical losses from the operation of traction motors can raise machine parts to temperatures as high as 108 ^{o}C [16], 140 ^{o}C [17], and 200 ^{o}C[18], depending on size, age, geometry, cooling and drive cycle. In the aforementioned papers, the high and low frequency characteristics of induction motors have been studied using data at room temperature and ECMs. ECMs are known for their limited flexibility [2] and this suggests that parameters estimated at certain temperatures could result in large errors as operating conditions and consequently parameters change especially when electric machines are used for traction.

In this paper the temperature dependent parameters of an equivalent circuit model have been estimated. This paper investigates the suitability of ECMs for studying machine behaviour at extreme temperature conditions and provides a valuable precursor to their application in modelling machine degradation, condition monitoring and advanced design. By considering temperature effects on motor model parameters, the universal induction per phase motor model proposed in [10] has been investigated. The approach uses impedance measurements acquired at the terminals (U, V, and W) of an induction machine over the temperature range T_R (room temperature) to 210 ^{o}C. Stator and rotor parameters are estimated across the temperature range using the Nelder-Mead simplex algorithm, which is a well-defined and widely used numerical method. There is a number of optimisation methods available, see [19]; however, estimation of ECM parameters can be easily transformed into

an unconstrained optimisation problem, hence it is believed that the simplex method is sufficient for this study. Using this framework, the temperature dependences of the various machine parameters have been analysed.

2 Background to induction machines

In recent years, induction machines have also found employment in electric vehicles, examples of these include the Tesla Roadster, General Motors EV-1, and AC Propulsion vehicles - Tzero technology which has been used in BMW Mini-E and Taiwan's Yulon MPV. While permanent magnet (PM) vehicle machines are becoming more predominant in electric vehicles, still many merits remain in favour of induction machines, most notably low cost, well proven technology and their inherent robustness. The particular machine used for this research was an Alpak11 AC induction motor, 0.37 kW, RPM 1460. This machine of course is a lot smaller than that found in an electric vehicle however in principle the theory and methodology still apply as the physics remain the same albeit appropriate parameter scaling in required.

3 Model description

In this paper, the equivalent circuit model (ECM) for an induction machine proposed by Mirafzal et al. [14] is investigated, see Figure 1 and Table 1. This circuit is sufficient for describing the impedance behaviour of an induction machine at both low and high frequencies [14], i.e. between 10 Hz and 10 MHz. The parameters L_{ls}, C_{sw}, C_{sf}, μR_s, and R_{sw} have

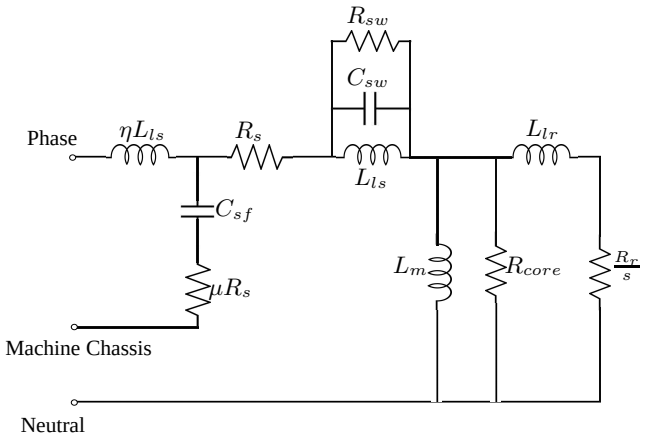

Figure 1: ECM of induction machine

been added to the conventional electric machine circuit, as presented in [11]. The stator resistance can be measured using a rated DC current [4]. The term μR_s, which is proportional to the stator resistance, is used to account for the first few turns nonlinear voltage gradient at high frequency. For wire wound motors, the current flowing in the stator induces electromotive force in the rotor windings which flows as the rotor is short-circuited. The damping resistance in winding represents the power losses which occur in the rotor winding. The stator first turn leakage inductance (ηL_{ls}) is defined by

$$\eta L_{ls} = \left(\frac{n_f}{n_t}\right)^2 L_{ls} \tag{1}$$

where n_f is the number of first few turns and n_t refers to the total number of turns per phase. The first turn stator leakage inductance is used to account for the first few turns affect on the high frequency anti resonance. The slip s is unity as the rotational speed of the rotor for the experiments is zero. This facilitates the estimation of R_r as a stand-alone parameter of the ECM.

Parameter	Description
R_s	stator resistance
R_r	rotor resistance
L_{lr}	rotor inductance
R_{core}	core loss resistance
L_m	magnetising inductance
L_{ls}	stator leakage inductance
ηL_{ls}	stator first turn leakage inductance
C_{sw}	stator turn to turn winding capacitance
C_{sf}	stator to frame capacitance
μR_s	stator to frame to ground damping resistance
R_{sw}	damping resistance in winding
s	slip

Table 1: Parameters of ECM

4 Experimental procedure

The experiment specimen i.e. the electric machine, was placed inside the laboratory oven as shown in Fig 3(a). Measurements of impedance for room temperature (22.4 $^\circ$C) were first made prior to activating the electric oven. The frequency range was 100 Hz – 20 MHz. The temperature of the oven was then increased to 30 $^\circ$C and thereafter increased at intervals of 20 $^\circ$C up to 210 $^\circ$C. An internal temperature sensor (thermocouple) was used to measure the specimen's temperature using a YCT Data Logger Thermometer (YC-747UD) and the impedance was measured using a N4L precision impedance/LCR analyser (PSM1735 with Impedance Analysis Interface) see Fig 3(b). The acquired impedance measurements for the three phases (U,V,W) are shown in Fig. 2(a) and 2(b) for magnitude and phase respectively.

5 Parameter estimation

The parameters of the ECM have been estimated for different values of the temperature (T) and are presented in the Appendix A in Tables 2-4. In order to obtain each parameter set a quadratic cost function has been minimised using the Nelder-Mead simplex method for nonlinear optimisation [20]. The model has been fitted for the frequency range 100 Hz-10 MHz.

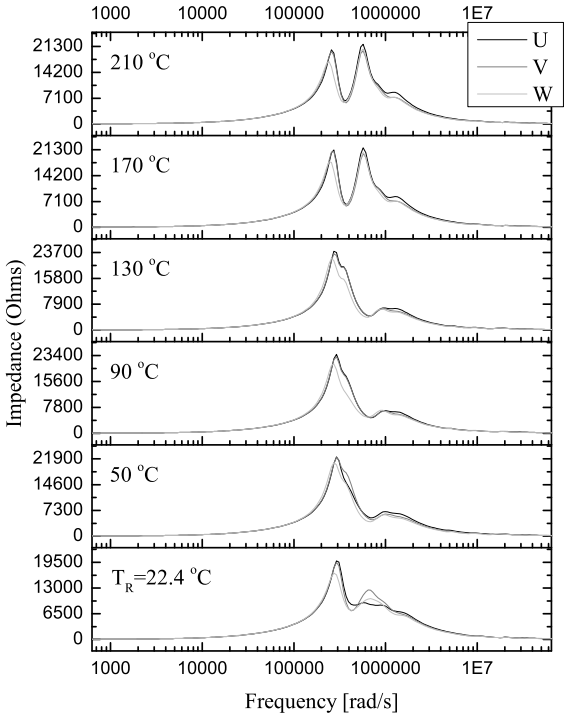

(a) Impedance (Magnitude)

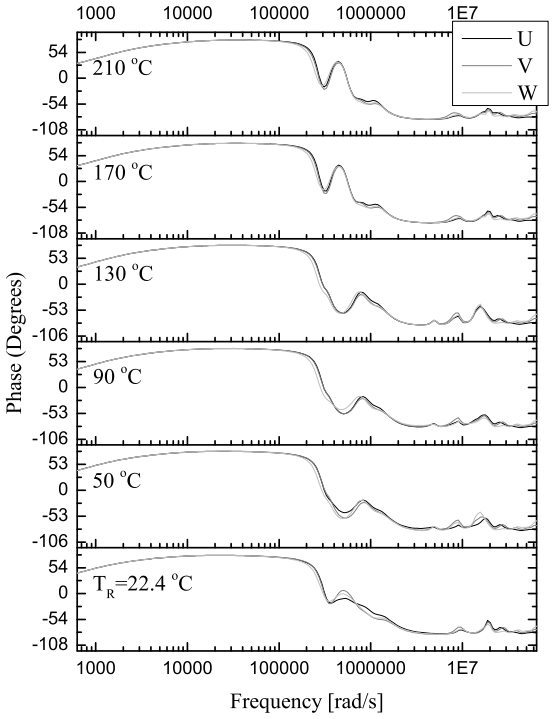

(b) Impedance (Phase)

Figure 2: Impedance measurements of the three phases (U, V, W) over the temperature range T_R to 210 °C

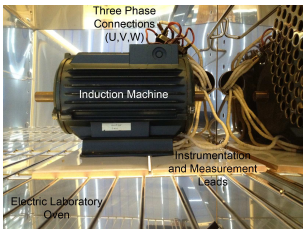

(a) Inside the electric oven

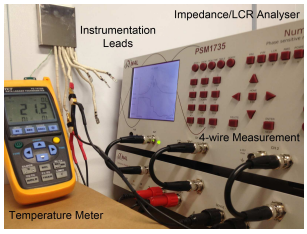

(b) Outside the oven with the laboratory equipment (Impedance LCR Analyser and Temperature Data Logger)

Figure 3: The experiment setup

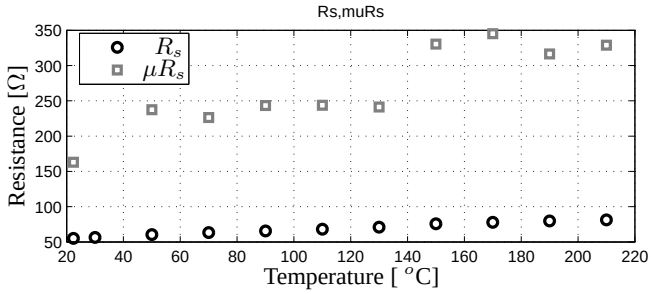

Figure 4: Dependency between temperature and identified values of R_s and μR_s

It is observed that R_s, R_{core}, ηR_s, and C_{cf} increase with an increase of the temperature, see Figures 4-6. This is to be expected as the resistance of the materials increases with temperature, non-linearly in this case as we are dealing with composite materials, e.g. laminated steel and polymer coated copper. Furthermore, some of the ECM parameters have outliers compared to those calculated for different temperatures, e.g. μR_s calculated for 30 ^{o}C. This might be due to noise in the data or some limitations in the optimisation method used. However, they have minimal influence on the overall analysis. Figures 7 and 8 present frequency responses of the ECM compared with the measured data for the two extreme temperature cases, i.e. 22.4 ^{o}C and 210 ^{o}C. The ECM can replicate both resonances and the anti-resonance when the temperature is relatively low, see Figure 7. One can note a third resonance in the measured data at approximately $2 \cdot 10^6$ rad/s, see phase plot of Figure 7, which appears to be not well accounted for by the model. This third resonance has relatively negligible effect on the frequency response of induction machine for $T \leq 130^o$C. However, as the temperature increases above 130 ^{o}C, the third resonance becomes more pronounced, see Figure 8. The evolution of these trends with respect to temperature was well presented in the impedance measurements in Figure 4. It would appear that the considered ECM model structure is insufficient for accurately modelling the induction machine over the spectrum considered. This might also explain a significant change in the trend of the

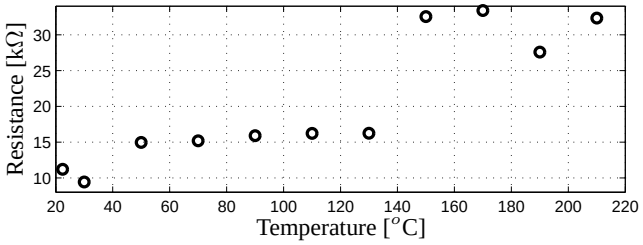

Figure 5: Dependency between temperature and identified value of R_{core}

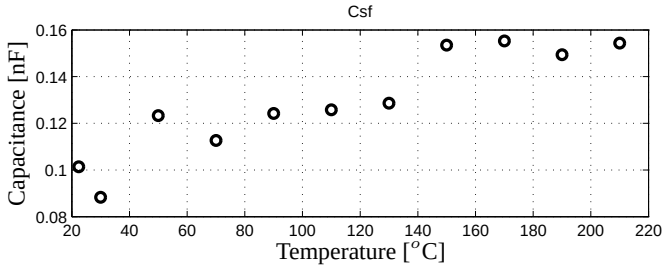

Figure 6: Dependency between temperature and identified value of C_{fs}

ECM parameters when the temperature increases above 130 ^{o}C such as, for example, a 'abrupt' shift upwards in R_{core}, see Figure 5, or a drop in R_{sw}, see Table 2 (note that R_{sw} increases with an increase of the temperature for $T \leq 130^o$C).

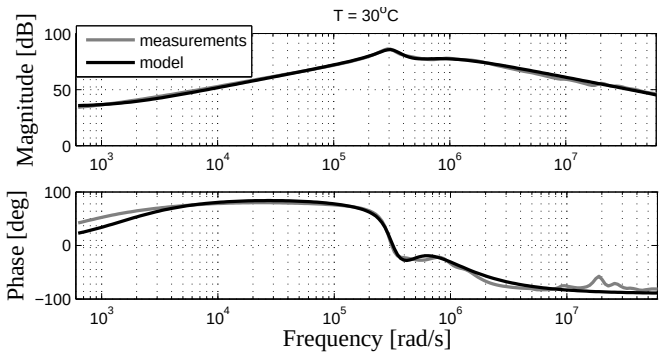

Figure 7: Frequency response of ECM compared with measured data for T $= 30^o$C

In order to assess the goodness of fit of the ECM, a quantitative efficacy index is required. In this paper average values of the absolute magnitude modelling error and absolute phase modelling error, expressed in, relatively, dB and deg, are used. The efficacy indices are calculated by substracting the magnitude (or phase) of the model from the measured magnitude (or phase) and then computing the absolute value. Then an average value of the absolute magnitude (or phase) error is compared for different temperatures, see Figure 9, or frequencies, see Figure 10. One can note a significant increase in both average absolute magnitude modelling error and average absolute phase modelling error when the temperature increases above 130 ^{o}C. This is probably due to the fact that the considered ECM is not sufficient for induction machine modelling in high temperatures. The average values of frequency response error plotted for different frequencies are presented in Figure 10. One can note that the ECM struggles to accurately describe the induction machine behaviour for relatively high frequencies (above 10^6 rad/s) which could be related to high frequency effects and associated parasitic elements e.g. from the measurement leads.

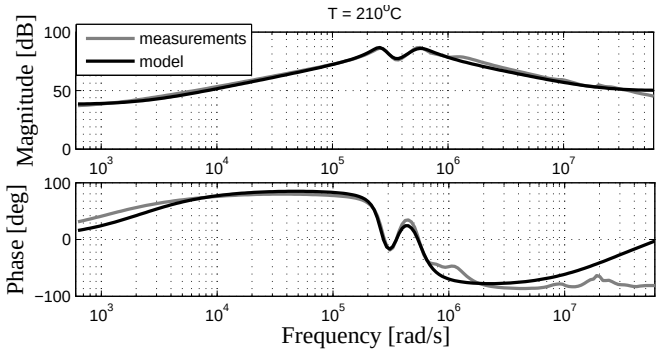

Figure 8: Frequency response of ECM compared with measured data for T $= 210^o$C

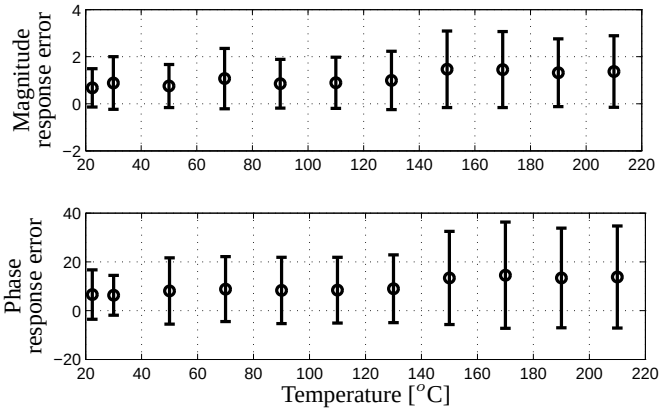

Figure 9: Uncertainty of ECM for different temperatures. Circles denote magnitude (top subfigure) and phase modelling errors (bottom subfigure), whilst error bars represent the standard deviation of magnitude and phase response error.

6 Conclusions and future work

In this paper the impact of temperature on the frequency response of the induction machine is considered. Based on experimental data, the parameters of the ECM, which has been originally developed by Mirafzal et al. [14, 21] for room temperature, are estimated for different values of the temperature

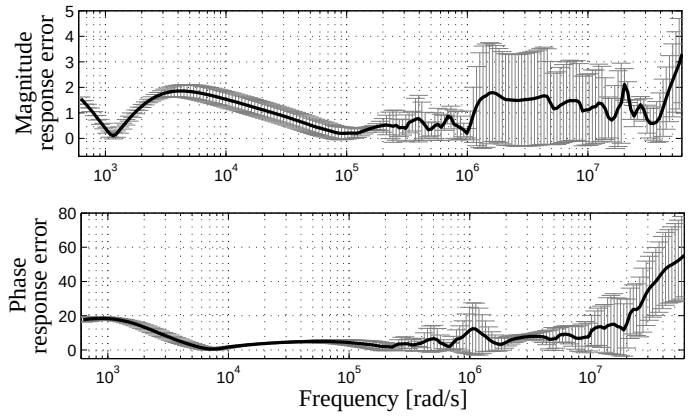

Figure 10: Accuracy of ECM for different frequencies. Black lines denote average of magnitude and phase estimation error (respectively, upper and lower subfigure), grey error bars represent standard deviation of magnitude and phase response error.

and their dependency on the temperature is evaluated.

It is observed that Mirafzal's et al. [14, 21] model can reproduce the two dominant resonances observed in the induction machine. As the third resonance has minor impact on the frequency response for low temperatures, the considered ECM exhibits good match with the measured data. However, as the temperature increases above 130 ^{o}C, the third resonance becomes significant and the considered ECM is not sufficient to replicate the behaviour of the induction machine. Thus the future work aims towards an extension of the ECM to incorporate effects of the third resonance.

It is also observed that with an increase of the temperature, the resonances move towards lower frequencies. This is due to a temperature related increase of capacitance (the parameter estimation reveals that the stator to frame capacitance increases with an increase of the temperature). Furthermore, the second and the third resonance become more pronounced in the spectrum when the temperature increases. It is observed that the resistance values such as the stator resistance, the core loss resistance, the damping resistance in winding, and the stator to frame to ground damping resistance exhibit an increasing trend upwards with an increase of temperature, which is an expected result. Some parameter estimates, such as the rotor inductance, the rotor resistance, the magnetic inductance, and the rotor inductance do not show clear correlation to the temperature and vary significantly from data set to data set. This may be either due to the fact that the considered ECM cannot reproduce the third resonance or because of the some limitation of optimisation approach used. Future work will explore the physical origin of the third resonance visible in the data and extending the ECM to incorporate its effects. Also it is planned to further investigate the optimisation of the parameter estimation, in particular, the robustness of the results to the algorithm initialisation.

Acknowledgements

This work is part of the EPSRC funded FUTURE Vehicles project (EP/I038586/1). The authors also acknowledge the support from project partners.

References

[1] L. Chang. "An improved Fe inductance calculation for electrical machines". *IEEE Transactions on Magnetics*, **32**(4), pp. 3237–3245, (1996).

[2] M. Yilmaz and P.T. Krein. "Capabilities of finite element analysis and magnetic equivalent circuits for electrical machine analysis and design". In *IEEE Power Electronics Specialists Conference*, pp. 4027–4033, (2008).

[3] D.G. Taylor. "Nonlinear control of electric machines: an overview". *IEEE Control Systems*, **14**(6), pp. 41–51, (1994).

[4] S.-B. Lee and T.G. Habetler. "An on-line stator winding resistance estimation technique for temperature monitoring of line-connected induction machines". In *Conference Record of the 2001 IEEE Industry Applications Conference. Thirty-Sixth IAS Annual Meeting*, **3**, pp. 1564–1571, (2001).

[5] N. Lahoud, J. Faucher, D. Malec, and P. Maussion. "Electrical ageing modeling of the insulation of low voltage rotating machines fed by inverters with the design of experiments (DoE) method". In *the 2011 IEEE International Symposium on Diagnostics for Electric Machines, Power Electronics Drives (SDEMPED)*, pp. 272–277, (2011).

[6] P.H. Mellor, D. Roberts, and D.R. Turner. "Lumped parameter thermal model for electrical machines of tefc design". *IEE Proceedings on Electric Power Applications*, 138(5), pp. 205–218, (1991).

[7] S.K. Chowdhury and P.K. Baski. "A simple lumped parameter thermal model for electrical machine of tefc design". In *2010 Joint International Conference on Power Electronics, Drives and Energy Systems (PEDES)* , pp. 1–7, (2010).

[8] S. Grubic, J.M. Aller, Bin Lu, and T.G. Habetler. "A survey on testing and monitoring methods for stator insulation systems of low-voltage induction machines focusing on turn insulation problems". *IEEE Transactions on Industrial Electronics*, **55**(12), pp. 4127–4136, (2008).

[9] J.P. Wang, D.K. Lieu, W.L. Lorimer, and A. Hartman. "Comparison of lumped parameter and finite element magnetic modeling in a brushless dc motor". *IEEE Transactions on Magnetics*, **33**(5), pp. 4092–4094, (1997).

[10] E.R. Lwithwaite. "Magnetic equivalent circuits for electrical machines". *Proceedings of the Institution of Electrical Engineers*, **114**(11), pp. 1805–1809, (1967).

[11] "IEEE standard test procedure for polyphase induction motors and generators, (2004)".

[12] G. Grandi, D. Casadei, and U. Reggiani. "Equivalent circuit of mush wound ac windings for high frequency analysis". In *Proceedings of the IEEE International Symposium on Industrial Electronics*, **1**, pap. 201–206, (1997).

[13] O.A. Mohammed, S. Ganu, N. Abed, Z. Liu, and S. Liu. "High frequency modeling of pm synchronous machine for use in integrated motor drive". In *IEEE Electric Ship Technologies Symposium* , pp. 245–249, (2007).

[14] B. Mirafzal, G.L. Skibinski, R.M. Tallam, D.W. Schlegel, and R.A. Lukaszewski. "Universal induction motor model with low-to-high frequency-response characteristics". *IEEE Transactions on Industry Applications*, **43**(5), pp. 1233–1246, (2007).

[15] H. Peng, Q. Wang, Y. Yang, and Z. An. "Modeling method of broadband equivalent circuit for motor". In *Sixth International Conference on Electromagnetic Field Problems and Applications (ICEF)*, pages 1–4, (2012).

[16] Li Cuiping, Pei Yulong, Ni Ronggang, and Cheng Shukang. "Analysis of 3d static temperature field of water cooling induction motor in mini electric vehicle". In *International Conference on Electrical Machines and Systems (ICEMS)*, pages 1–5, (2011).

[17] R. Rothe and K. Hameyer. "Life expectancy calculation for electric vehicle traction motors regarding dynamic temperature and driving cycles". In *IEEE International Electric Machines Drives Conference (IEMDC)* , pages 1306–1309, (2011).

[18] R. W. Finholt. "Thermal stability of a new insulating material used in traction motors". *American Institute of Electrical Engineers, Part II: Applications and Industry, Transactions of the*, **74**(1), pp. 37–41, (1955).

[19] C.B Gupta. *Optimization Techniques in Operational Research*, International Publishing House, (2007).

[20] J.C. Lagarias, J.A. Reeds, M.H. Wright, and P.E. Wright. "Convergence properties of the nelder-mead simplex method in low dimensions". *SIAM Journal of Optimization*, **9**, pp. 112–147, (1998).

[21] B. Mirafzal, G.L. Skibinski, and R.M. Tallam. "Determination of parameters in the universal induction motor model". *IEEE Transactions on Industry Applications*, **45**(1), pp. 142–151, (2009).

A Appendix

T	R_s	R_{sw}	R_{core}	R_r
^oC	$[\Omega]$	$[\Omega \cdot 10^4]$	$[\Omega \cdot 10^4]$	$[\Omega \cdot 10^{-2}]$
22.4	55.0485	1.0469	1.1206	1.0368
30	56.3303	1.2055	0.9435	0.7392
50	60.5227	1.5521	1.4965	0.1975
70	63.2201	1.8157	1.5183	0.0796
90	65.6394	1.7606	1.5902	0.4540
110	68.1442	1.8150	1.6219	0.5452
130	70.9117	1.8923	1.6247	0.3496
150	75.6405	1.1562	3.2548	0.3568
170	77.8610	1.1746	3.3406	10.9382
190	79.8117	1.1548	2.7581	0.0016
210	81.2084	1.1303	3.2347	12.2169

Table 2: Parameters of ECM for different values of T

T	L_{ls}	L_{lr}	L_m
^oC	$[\text{H}\cdot 10^{-3}]$	$[\text{H}\cdot 10^{-2}]$	$[\text{H}\cdot 10^{-1}]$
22.4	9.3507	7.9553	0.4522
30	15.5113	2.6162	1.5841
50	25.6991	2.2389	0.2159
70	26.8066	3.2304	0.1453
90	26.4664	10.5022	0.1189
110	26.7247	1.7557	0.2736
130	26.9767	1.6453	0.3053
150	12.2804	3.7113	0.6480
170	12.4184	3.0820	1.0452
190	12.3318	14.1357	0.2979
210	12.5575	2.5017	9.1609

Table 3: Parameters of ECM for different values of T

T	C_{sw}	C_{sf}	μR_s	ηL_{ls}
^oC	$[\text{F}\cdot 10^{-10}]$	$[\text{F}\cdot 10^{-10}]$	$[\Omega \cdot 10^2]$	$[\text{H}\cdot 10^{-8}]$
22.4	9.8250	1.0135	1.6298	$1.5\cdot 10^{-8}$
30	5.5450	0.8832	$9.9\cdot 10^{-13}$	7.1480
50	2.6201	1.2327	2.3731	17.6480
70	2.5432	1.1266	2.2624	47.0667
90	2.5731	1.2421	2.4337	17.6925
110	2.5968	1.2578	2.4381	7.1398
130	2.6577	1.2863	2.4130	14.0178
150	9.1288	1.5352	3.3039	4.7499
170	9.2301	1.5528	3.4513	163.0242
190	9.6399	1.4941	3.1648	150.9447
210	9.6814	1.5438	3.2879	149.6282

Table 4: Parameters of ECM for different values of T